

<https://helda.helsinki.fi>

---

## The PNPLA3-I148M variant increases polyunsaturated triglycerides in human adipose tissue

Qadri, Sami

2020-08-12

---

Qadri , S , Lallukka-Brück , S , Luukkonen , P K , Zhou , Y , Gastaldelli , A , Orho-Melander , M , Sammalkorpi , H , Juuti , A , Penttilä , A K , Perttilä , J , Hakkarainen , A , Lehtimäki , T E , Oresic , M , Hyötyläinen , T , Hodson , L , Olkkonen , V M & Yki-Järvinen , H 2020 , ' The PNPLA3-I148M variant increases polyunsaturated triglycerides in human adipose tissue ' , Liver International , vol. 40 , no. 9 , pp. 2128-2138 . <https://doi.org/10.1111/liv.14507>

---

<http://hdl.handle.net/10138/333732>

<https://doi.org/10.1111/liv.14507>

---

acceptedVersion

---

*Downloaded from Helda, University of Helsinki institutional repository.*

*This is an electronic reprint of the original article.*

*This reprint may differ from the original in pagination and typographic detail.*

*Please cite the original version.*

DR. SAMI QADRI (Orcid ID : 0000-0001-9313-9324)

DR. AMALIA GASTALDELLI (Orcid ID : 0000-0003-2594-1651)

Article type : Original Articles

Corresponding Author Email ID: sami.qadri@helsinki.fi

## **The PNPLA3-I148M variant increases polyunsaturated triglycerides in human adipose tissue**

Sami Qadri<sup>1,2</sup>, Susanna Lallukka-Brück<sup>1,2</sup>, Panu K. Luukkonen<sup>1,2</sup>, You Zhou<sup>2,3</sup>, Amalia Gastaldelli<sup>4</sup>, Marju Orho-Melander<sup>5</sup>, Henna Sammalkorpi<sup>6</sup>, Anne Juuti<sup>6</sup>, Anne K. Penttilä<sup>6</sup>, Julia Perttilä<sup>2</sup>, Antti Hakkarainen<sup>7</sup>, Tiina E. Lehtimäki<sup>7</sup>, Matej Orešič<sup>8</sup>, Tuulia Hyötyläinen<sup>8</sup>, Leanne Hodson<sup>9</sup>, Vesa M. Olkkonen<sup>2</sup>, Hannele Yki-Järvinen<sup>1,2</sup>

<sup>1</sup>Department of Medicine, University of Helsinki and Helsinki University Hospital, Helsinki, Finland; <sup>2</sup>Minerva Foundation Institute for Medical Research, Helsinki, Finland; <sup>3</sup>Systems Immunity University Research Institute and Division of Infection and Immunity, School of Medicine, Cardiff University, Cardiff, United Kingdom; <sup>4</sup>Institute of Clinical Physiology, National Research Council, Pisa, Italy; <sup>5</sup>Department of Clinical Sciences, Diabetes and Endocrinology, University Hospital Malmö, Lund University, Malmö, Sweden; <sup>6</sup>Department of Gastrointestinal Surgery, Helsinki University Hospital, Abdominal Center, Helsinki, Finland; <sup>7</sup>HUS Medical Imaging Center, Helsinki University Hospital, Helsinki, Finland; <sup>8</sup>Department of Chemistry, Örebro University, Örebro, Sweden; <sup>9</sup>Oxford Centre for Diabetes, Endocrinology and Metabolism, University of Oxford and National Institute for Health Research Oxford Biomedical Research Centre, Oxford University Hospitals Foundation Trust, Oxford, United Kingdom.

**Word count:** Abstract 250; Main body 4957

This article has been accepted for publication and undergone full peer review but has not been through the copyediting, typesetting, pagination and proofreading process, which may lead to differences between this version and the [Version of Record](#). Please cite this article as [doi: 10.1111/liv.14507](https://doi.org/10.1111/liv.14507)

This article is protected by copyright. All rights reserved

**Number of figures and tables:** 3 figures and 1 table. 4 supplementary figures and 5 supplementary tables.

## **ABBREVIATIONS**

PNPLA3, patatin like phospholipase domain containing 3; NAFLD, non-alcoholic fatty liver disease; TG, triglyceride; PUFA, polyunsaturated fatty acid; NEFA, non-esterified fatty acid; AT, adipose tissue; IHTG, intrahepatic triglyceride; FA, fatty acid; <sup>1</sup>H-MRS, proton magnetic resonance spectroscopy; HbA<sub>1c</sub>, hemoglobin A<sub>1c</sub>; LDL, low-density lipoprotein; HDL, high-density lipoprotein; ALT, alanine aminotransferase; AST, aspartate aminotransferase; GGT, gamma-glutamyl transferase; UHPLC-QTOF-MS, ultra-high performance liquid chromatography-quadrupole time-of-flight mass spectrometry; GC, gas chromatography; FAME, fatty acid methyl ester; GC×GC/TOFMS, comprehensive two-dimensional gas chromatography time-of-flight mass spectrometry; RT-qPCR, real-time quantitative polymerase chain reaction; SDS, sodium dodecyl sulfate; BCA, bicinchoninic acid; ECL enhanced chemiluminescence; FDR, false discovery rate; R<sub>a</sub>, rate of appearance; DPA, docosapentaenoic acid; AA, arachidonic acid; PC, phosphatidylcholine

## **CONFLICTS OF INTEREST**

The authors have declared that no conflicts of interest exist.

## **FINANCIAL SUPPORT**

This study was supported by research grants from the Academy of Finland (HY grant no. 309263), the EU H2020 project 'Elucidating Pathways of Steatohepatitis' (HY, TH, MO: EPoS grant no. 634413), and the H2020-JTI-IMI2 EU project 777377-2 Liver Investigation: Testing Marker Utility in Steatohepatitis (LITMUS) (HY, TH, MO) and the Sigrid Juselius (HY, PL), EVO (HY) and the Novo Nordisk (HY, PL) Foundations. LH is a British Heart Foundation Senior Research Fellow in Basic Science (FS/15/56/31645).

## **ACKNOWLEDGEMENTS**

We gratefully acknowledge volunteers for their help. We thank Aila Karioja-Kallio, Päivi Ihamuotila and Mia Urjansson for their excellent technical assistance.

## ABSTRACT

**Background & Aims:** The I148M variant in PNPLA3 is the major genetic risk factor for non-alcoholic fatty liver disease (NAFLD). The liver is enriched with polyunsaturated triglycerides (PUFA-TGs) in PNPLA3-I148M carriers. Gene expression data indicate that PNPLA3 is liver-specific in humans, but whether it functions in adipose tissue (AT) is unknown. We investigated whether PNPLA3-I148M modifies AT metabolism in human NAFLD.

**Methods:** Profiling of the AT lipidome and fasting serum non-esterified fatty acid (NEFA) composition were conducted in 125 volunteers (*PNPLA3*<sup>I148M/M1</sup>, *n*=63; *PNPLA3*<sup>I148II</sup>, *n*=62). AT fatty acid composition was determined in 50 volunteers homozygous for the variant (*PNPLA3*<sup>I148MM</sup>, *n*=25) or lacking the variant (*PNPLA3*<sup>I148II</sup>, *n*=25). Whole-body insulin sensitivity of lipolysis was determined using [<sup>2</sup>H<sub>5</sub>]glycerol, and PNPLA3 mRNA and protein levels were measured in subcutaneous AT and liver biopsies in a subset of the volunteers.

**Results:** PUFA-TGs were significantly increased in AT in carriers versus non-carriers of PNPLA3-I148M. The variant did not alter the rate of lipolysis or the composition of fasting serum NEFAs. *PNPLA3* mRNA was 33-fold higher in the liver than in AT (*p*<0.0001). In contrast, PNPLA3 protein levels per tissue protein were 3-fold higher in AT than the liver (*p*<0.0001) and 9-fold higher when related to whole-body AT and liver tissue masses (*p*<0.0001).

**Conclusions:** Contrary to previous assumptions, PNPLA3 is highly abundant in AT. PNPLA3-I148M locally remodels AT TGs to become polyunsaturated as it does in the liver, without affecting lipolysis or composition of serum NEFAs. Changes in AT metabolism do not contribute to NAFLD in PNPLA3-I148M carriers.

## Keywords

adipose tissue, fatty acids, lipidomics, lipolysis, non-alcoholic fatty liver disease, triglycerides

## Lay Summary

The common I148M variant in the gene *PNPLA3* is the main genetic risk factor for fatty liver disease, but whether the variant protein exists or alters lipid metabolism in human adipose tissue is unknown. We found that the PNPLA3 protein is found at high concentrations in human adipose tissue and that carriers of the PNPLA3-I148M variant have changes in their adipose tissue lipid composition that mirror those seen in the liver.



## INTRODUCTION

A common nonsynonymous single-nucleotide polymorphism (rs738409; c.444C>G, p.I148M) in the patatin like phospholipase domain containing 3 (*PNPLA3*, adiponutrin) gene was found in the Dallas Heart Study to significantly increase liver fat content in three different ethnic groups<sup>1</sup>. This finding has since been extensively replicated<sup>2</sup>. The I148M allele is found in 30-50% of all subjects<sup>3,4</sup> and increases the risk of both alcoholic and non-alcoholic fatty liver disease (NAFLD), including cirrhosis and hepatocellular carcinoma<sup>5</sup>.

In contrast to NAFLD associated with insulin resistance and metabolic syndrome, in which the steatotic liver mainly consists of saturated fat, the human liver lipidome is characterized by absolute and relative increases in polyunsaturated triglycerides (TGs) in *PNPLA3*-I148M variant carriers compared with non-carriers<sup>6</sup>. The I148M variant increases polyunsaturated fatty acid (PUFA) retention in liver TGs and decreases incorporation of PUFAs into phospholipids<sup>7</sup>. These data closely resemble those of knock-in mice expressing a catalytically inactive form of *PNPLA3* in the liver (*PNPLA3*-S47A)<sup>8</sup>. Non-esterified fatty acids (NEFAs) resulting from adipose tissue (AT) lipolysis are the main source of intrahepatic triglycerides (IHTGs) in NAFLD<sup>9</sup>. There are no data on whether *PNPLA3*-I148M exerts changes in the lipid composition of AT, as it does in the liver<sup>6,7</sup>. Moreover, the potential impact of the I148M variant on AT lipolysis or the composition of NEFAs released from AT has not been studied.

Of interest, *PNPLA3* (previously known as adiponutrin) was initially discovered in mice as a nutritionally regulated transmembrane protein thought to be specific to the adipocyte lineage<sup>10,11</sup>. In humans the *PNPLA3* transcript is, in contrast to findings in mice and rats<sup>12-14</sup>, much more abundant in the liver than in AT<sup>15,16</sup>. Concentrations of the *PNPLA3* protein in the human liver or AT have not, however, been previously studied. This would be important as efforts are currently ongoing to find therapeutic targets for the treatment of advanced NAFLD in genetically predisposed patients<sup>17-19</sup>.

In the present study, we investigated whether the human AT lipidome is modified in a polyunsaturated direction in carriers of *PNPLA3*-I148M compared with non-carriers, as it is in the liver. Since this was found to be the case, we next examined whether the variant affects AT lipolysis or the composition of circulating NEFAs. In addition, we compared *PNPLA3* mRNA and protein levels between human liver and subcutaneous AT in a subset of the volunteers.

## MATERIALS AND METHODS

### Volunteers and study design

*Effects of PNPLA3-I148M on AT TG and serum NEFA composition.* We profiled the AT lipidome and fasting serum NEFA composition in 125 consecutive patients undergoing laparoscopic bariatric surgery who fulfilled the following inclusion criteria: (i) age 18–75 years; (ii) no known acute or chronic disease except for obesity, type 2 diabetes, NAFLD or hypertension on the basis of history, physical examination, electrocardiogram, and standard laboratory tests (complete blood count, serum creatinine, electrolyte concentrations); (iii) alcohol consumption <20 g per day for women and <30 g per day for men; (iv) no clinical or biochemical evidence of liver disease other than NAFLD (such as hepatitis B or C), or clinical signs or symptoms of inborn errors of metabolism; (v) no history of use of drugs or toxins influencing liver steatosis; (vi) not pregnant or lactating. We have previously reported data on the liver lipidome in a cohort that mostly consisted of the same volunteers<sup>6,7</sup>. The present cohort differs slightly from that published earlier (119 shared volunteers) due to technical issues in a few of the lipidomic analyses. The volunteers participated in a clinical research visit prior to surgery and underwent liver and AT biopsies at the time of bariatric surgery (*vide infra*). PNPLA3 mRNA and protein levels between liver and AT samples were compared in a subset of 20 of these volunteers, who had enough liver tissue left after histologic and lipidomic analyses.

*Effects of PNPLA3-I148M on AT fatty acid composition and inflammation.* In addition to the AT lipidome profiling described above, we examined the composition of AT fatty acids (FAs) and compared gene expression of several proinflammatory (*MCP-1*, *CD68*) and anti-inflammatory (*Twist1*, *ADIPOQ*) markers in AT in a separate group of 50 volunteers who did not undergo bariatric surgery and were known to be homozygous (*PNPLA3*<sup>148II</sup>, *n*=25; *PNPLA3*<sup>148MM</sup>, *n*=25) based on previous genotyping results. The inclusion criteria were as listed above. The volunteers participated in a clinical research visit during which needle biopsies of abdominal AT were also obtained (*vide infra*). In addition, on a separate visit, liver IHTG content was measured by proton magnetic resonance spectroscopy (<sup>1</sup>H-MRS).

*Effects of PNPLA3-I148M on in vivo AT lipolysis.* We recruited 28 non-diabetic volunteers by contacting participants of prior metabolic studies who were known to be homozygous (*PNPLA3*<sup>148II</sup>, *n*=19; *PNPLA3*<sup>148MM</sup>, *n*=9) based on previous genotyping results. The inclusion criteria were as listed above. These volunteers participated in a clinical research visit as well as in a metabolic study during which whole-body lipolysis was measured using [<sup>2</sup>H<sub>5</sub>]glycerol in the basal state and during euglycemic hyperinsulinemia (*vide infra*). In addition, on a separate visit, liver IHTG content was measured by <sup>1</sup>H-MRS.

The study was conducted in accordance with the Declaration of Helsinki. Each participant provided a written informed consent after being explained the nature and potential risks of the study. The ethics committee of the Helsinki University Hospital approved the studies.

### **Clinical research visit**

The volunteers arrived in the clinical research center after an overnight fast (one week prior to surgery for the bariatric surgery volunteers). At this visit, a history and physical examination were performed and fasting blood samples were withdrawn for measurement of concentrations of glucose, HbA<sub>1c</sub>, insulin, lipids, liver enzymes, and creatinine and for genotyping of *PNPLA3* as previously described<sup>20</sup>. Total liver mass was determined from an equation we have previously developed<sup>21</sup>.

### **Adipose tissue and liver biopsies**

Immediately at the beginning of the laparoscopic bariatric surgery procedure, a wedge biopsy of the liver was taken in addition to a subcutaneous abdominal AT biopsy. The AT sample and approximately one-half of the liver sample were immediately snap-frozen in liquid nitrogen and stored at -80 °C until subsequent analysis of molecular lipids. The time from obtaining the biopsies until freezing the samples in liquid nitrogen was approximately one minute. The remainder of the liver biopsy was sent to the pathologist for routine histopathological assessment using the criteria proposed by Brunt *et al.*<sup>22</sup>. For the non-surgical volunteers, needle aspiration biopsy specimens of subcutaneous

abdominal AT were taken under local anesthesia with 1% lidocaine at the clinical research visit as previously described<sup>23</sup>.

### **Lipidomic analysis**

The AT lipidome was analyzed using an ultra-high performance liquid chromatography-quadrupole time-of-flight mass spectrometry system (UHPLC-QTOF-MS; Agilent Technologies, Santa Clara, CA). In addition to TGs, the analysis covered most of the major molecular lipids including ceramides, sphingomyelins, phosphatidylcholines, phosphatidylethanolamines, and lysophosphatidylcholines. For detailed methodology, see Supporting Information.

### **Composition of AT FAs**

The analysis of AT FA composition was performed using gas chromatography (GC). AT lipids were extracted according to the method of Folch *et al.*<sup>24</sup>. The TG fraction was separated by solid-phase extraction<sup>25</sup> and fatty acid methyl esters (FAMES) prepared and analyzed by GC<sup>26</sup>. FAs were identified using a standard containing FAMES ranging from chain length 6 to 24 (Sigma-Aldrich Company Ltd, Poole, Dorset, UK). A FAME standard of known composition (AOCS std#6, Thames Restek UK Ltd, Saunderton, Bucks, UK) and a quality control sample (mixture of fatty acids [Sigma-Aldrich Company Ltd] and TGTG [MaxEPA fish oil, Seven Seas Ltd, Marfleet, Hull UK]) were run alongside each batch of samples to check correct peak identification and instrument performance. GC results were converted to mol %.

### **Composition of fasting serum NEFAs**

The analysis of NEFAs was done using comprehensive two-dimensional gas chromatography time-of-flight mass spectrometry (GC×GC/TOFMS; Pegasus 4D, Leco Corp., St. Joseph, MI), as described previously in detail<sup>27</sup> and outlined in Supporting Information.

### **Insulin sensitivity of whole-body AT lipolysis**

The rate of whole-body lipolysis was measured basally after an overnight fast and during intravenously maintained euglycemic hyperinsulinemia by infusing [<sup>2</sup>H<sub>5</sub>]glycerol as

previously described<sup>28</sup>. The basal and insulin infusion periods both lasted 120 min, and the rate of the continuous insulin infusion was 0.4 mU·kg<sup>-1</sup>·min<sup>-1</sup>. The low insulin infusion rate was chosen to maximize the likelihood of detecting changes in lipolysis<sup>29</sup>.

### Measurement of IHTGs

In the 28 volunteers in whom *in vivo* lipolysis was measured, and in the 50 volunteers from whom a needle biopsy of AT was obtained, IHTG content was measured by <sup>1</sup>H-MRS, as described<sup>30</sup>. To facilitate comparison between spectroscopic and histologic IHTG measurements, spectroscopic fat percentages were converted to correspond those obtained by liver biopsy using an equation we have previously published<sup>31</sup>.

### Messenger RNA expression

Real-time quantitative polymerase chain reaction (RT-qPCR) was performed on reverse-transcribed mRNA isolated from liver and AT samples, as described in Supporting Information.

### Protein levels

Immunoblotting was performed on protein lysates from subcutaneous AT and liver tissue specimens. Liver biopsies weighed from 11 to 37 mg (23±2 mg), and AT biopsies from 121 to 295 mg (187±10 mg). As a positive control, human *PNPLA3* cDNA in a pcDNA4HisMax-C vector (Invitrogen/Thermo Scientific, Carlsbad, CA) was transfected into human hepatoma (HuH7) cells using Lipofectamine 2000 (Invitrogen), and total cell lysates were harvested at 24 h post-transfection<sup>32</sup>. For protein extraction, tissue samples were homogenized in Precellys®24 lysing tubes (Bertin Technologies, France) using 400 µl of lysis buffer containing 50 mM Tris-HCl, pH 7.4, 150 mM NaCl, 1% NP-40, 0.1% SDS and protease inhibitor cocktail (Roche Diagnostics, Basel, Switzerland). Protein concentrations were measured using the bicinchoninic acid (BCA) assay (Thermo Fisher Scientific, Waltham, MA). Proteins (30 µg/well) were separated on 10% SDS-polyacrylamide gels and transferred to nitrocellulose membranes, which were probed with antibodies against human *PNPLA3* (SAB1401851; Sigma-Aldrich) or β-actin (A2066; Sigma-Aldrich). The bound antibodies were detected with enhanced chemiluminescence

(ECL; Thermo Fisher Scientific). PNPLA3 band intensities were normalized to the band intensities of  $\beta$ -actin, which were analyzed from the same membranes.

## Statistics

Analyses were performed with Statistical Package for the Social Sciences (SPSS) version 25 (IBM Corporation, Armonk, NY) and GraphPad Prism version 7.04 (GraphPad Software, La Jolla, CA). The Shapiro-Wilk test was used to assess continuous variables for normality. We compared two independent groups using the unpaired Student's *t*-test or the Mann-Whitney *U* test for normally and non-normally distributed variables, respectively. We used the Pearson's  $\chi^2$  test or the Fisher's exact test as appropriate to evaluate if distribution of categorical variables differed between two groups. To compare gene and protein expression in AT and liver biopsies from the same volunteers, we used the paired *t*-test.  $\Delta C_t$  values were used in statistical analyses of the RT-qPCR data. For statistical analysis of AT lipidomic and serum NEFA composition data, missing values were imputed using half mean plus a very small amount of random noise. Lipid species with missing values in more than 50% of samples were excluded from analyses. Lipidomic data were  $\log_2$ -transformed before statistical hypothesis testing, and the Benjamini-Hochberg procedure<sup>33</sup> was applied to control false discovery rate (FDR) at a preselected level of  $Q=20\%$ . We report unadjusted *p* values for findings that are determined as discoveries. Otherwise, a *p* value of less than 0.05 was considered statistically significant. Sample size and power calculations are described in Supporting Information.

We have previously shown highly significant differences in lipidomic profiles of the liver between PNPLA3-I148M carriers (genotype CG or GG) and non-carriers in a sample of 125 volunteers. This justifies the similar sample size used for the AT and serum analyses, and the comparison of AT FA composition between 25 homozygous carriers and 25 non-carriers. Regarding the lipolysis study, interindividual variability in insulin suppression of glycerol  $R_a$  was determined based on data we have previously acquired in obese volunteers<sup>34</sup>. Based on these data we calculated that 9 homozygous carriers and 19 non-carriers are needed to detect a 14% between-group difference in insulin suppression of glycerol rate of appearance ( $R_a$ ) using a 2-sided *t*-test with a  $\beta$  value of 0.80 and an  $\alpha$  value of 0.05. Power calculations were performed using G\*Power 3.1.9.6<sup>35</sup>.

## RESULTS

### The AT lipidome is enriched with polyunsaturated TGs in PNPLA3-I148M variant carriers

Clinical characteristics of the 125 volunteers in whom lipidomic analyses of AT were conducted are shown in Table 1. The 63 carriers (*PNPLA3*<sup>148MM/MI</sup>) were similar to the 62 non-carriers (*PNPLA3*<sup>148II</sup>) with respect to sex, BMI, body fat, liver fat, and circulating concentrations of glucose, HbA<sub>1C</sub>, insulin, TG, and HDL and LDL cholesterol. Body weight of the bariatric surgery volunteers was similar at the time of the clinical research visit and surgery (130±2 kg vs. 128±2 kg, NS).

Absolute and relative concentrations of polyunsaturated TGs containing 5 to 9 double bonds were significantly higher in the *PNPLA3*<sup>148MM/MI</sup> group compared with the *PNPLA3*<sup>148II</sup> group, suggesting that PUFAs are enriched in TGs in AT of I148M variant carriers (Figure 1A, Supplementary Table 2). The number of double bonds in TGs were significantly positively correlated with the ratio of absolute TG concentrations between the groups (Figure 1B). A total of 14 individual polyunsaturated TG species were significantly increased in the *PNPLA3*<sup>148MM/MI</sup> group (Figure 1C), while we did not observe significant changes in saturated TGs. The results were reproduced when excluding volunteers with type 2 diabetes from analyses (Supplementary Figure 1). Previous lipidomic analysis of the liver in mostly the same volunteers showed similar PUFA enrichment in liver TGs of PNPLA3-I148M carriers<sup>6</sup>. We did not observe changes in concentrations of ceramides, sphingomyelins, lysophosphatidylcholines, phosphatidylcholines or phosphatidylethanolamines between the groups (Supplementary Table 3).

We conducted a further analysis of the composition of medium- to very long-chain FAs in AT samples of homozygous volunteers (*PNPLA3*<sup>148II</sup>, *n*=25; *PNPLA3*<sup>148MM</sup>, *n*=25). The groups were similar with respect to age, sex, BMI, and metabolic parameters (Supplementary Table 4). As a whole, there were no significant changes in saturated or monounsaturated FAs between the groups. We observed a significant increase in the relative abundance of the omega-3 PUFA docosapentaenoic acid (DPA, 22:5n-3; *p*=0.028) and a concomitant decrease in the omega-6 PUFA arachidonic acid (AA, 20:4n-

6;  $p=0.047$ ) in  $PNPLA3^{148MM}$  compared with  $PNPLA3^{148II}$  volunteers (Supplementary Figure 2). The omega-6 to omega-3 ratio was significantly decreased in the  $PNPLA3^{148MM}$  group compared with the  $PNPLA3^{148II}$  group ( $4.59\pm0.20$  vs.  $5.25\pm0.17$ ,  $p=0.013$ ). As with TGs, we observed a significantly positive correlation between the number of double bonds in FAs and the ratio of relative FA concentrations between the groups ( $r=0.50$ ,  $p=0.028$ , Supplementary Figure 3).

After observing the changes in PUFA-composition of AT FAs, we analyzed mRNA concentrations of pro- and anti-inflammatory genes in AT from the same volunteers. Levels of proinflammatory *CD68* ( $1.00\pm0.14$  vs.  $1.16\pm0.16$  AU) and *MCP-1* ( $1.00\pm0.10$  vs.  $0.89\pm0.09$  AU) mRNA were unchanged (all  $p>0.05$ ), whereas levels of anti-inflammatory *Twist1* ( $1.00\pm0.13$  vs.  $1.58\pm0.16$  AU,  $p=0.01$ ) and *ADIPOQ* ( $1.00\pm0.10$  vs.  $1.57\pm0.38$  AU,  $p=0.04$ ) were significantly increased in  $PNPLA3^{148MM}$  vs.  $PNPLA3^{148II}$  volunteers.

### ***In vivo* AT lipolysis or fasting serum NEFA composition are not affected in $PNPLA3$ -I148M variant carriers**

Clinical characteristics of the 28 volunteers in whom whole-body lipolysis was measured are shown in Table 1. The 9 homozygous carriers ( $PNPLA3^{148MM}$ ) were similar to the 19 non-carriers ( $PNPLA3^{148II}$ ) with respect to age, sex, BMI, body fat, liver fat, and circulating concentrations of glucose, HbA<sub>1c</sub>, insulin, TG, and HDL and LDL cholesterol.

Whole-body [<sup>2</sup>H<sub>5</sub>]glycerol  $R_a$  in the basal state was  $2.57\pm0.44$   $\mu\text{mol}\cdot\text{kg}^{-1}\cdot\text{min}^{-1}$  in the  $PNPLA3^{148MM}$  group and  $3.02\pm0.14$   $\mu\text{mol}\cdot\text{kg}^{-1}\cdot\text{min}^{-1}$  in the  $PNPLA3^{148II}$  group, with no significant difference between the groups ( $p>0.05$ , Figure 2A). During euglycemic hyperinsulinemia, glycerol  $R_a$  decreased to  $1.51\pm0.22$   $\mu\text{mol}\cdot\text{kg}^{-1}\cdot\text{min}^{-1}$  in the  $PNPLA3^{148MM}$  group, and similarly to  $1.56\pm0.08$   $\mu\text{mol}\cdot\text{kg}^{-1}\cdot\text{min}^{-1}$  in the  $PNPLA3^{148II}$  group ( $p>0.05$ , Figure 2B). The percentage suppression of glycerol  $R_a$  (i.e. lipolysis) by insulin did not significantly differ between  $PNPLA3^{148MM}$  and  $PNPLA3^{148II}$  volunteers ( $43.3\pm5.0$  vs.  $47.6\pm2.4$  %,  $p>0.05$ ) (Figure 2C).

We profiled the composition of fasting serum NEFAs in the same 125 volunteers in whom lipidomic studies of AT were conducted, as described above. After correcting for multiple



testing, we found no significant differences in absolute or relative concentrations of fasting serum NEFAs between the *PNPLA3*<sup>148MM/MI</sup> and *PNPLA3*<sup>148II</sup> groups (Supplementary Table 5).

**Expression of *PNPLA3* mRNA is markedly higher in the liver compared to AT, but the *PNPLA3* protein is more abundant in AT**

The change we observed in the AT lipidome in carriers of *PNPLA3*-I148M was unexpected as mRNA expression has been shown to be very low in human AT as compared to the liver<sup>15,16</sup>. There are, however, no protein data available. Therefore, we investigated *PNPLA3* protein levels in tissue samples of AT and the liver in a subset of 20 volunteers (mean age 46.0±1.9 years, mean BMI 45.6±1.4 kg/m<sup>2</sup>).

Quantitative PCR analysis showed that *PNPLA3* mRNA expression was markedly higher in the liver compared to AT. Normalized to the mRNA levels of the reference genes *36B4* and *ACTB*, expression of *PNPLA3* mRNA was on average 33-fold higher in the liver than in AT ( $p<0.0001$ ) (Figure 3A).

*PNPLA3* antibody specificity was confirmed by immunoblotting mock-transfected HuH7 cell lysates and cells transfected with *PNPLA3* (Supplementary Figure 4). Immunoblotting (Figure 3B) revealed that the level of *PNPLA3* protein was 3-fold higher in AT than the liver ( $p<0.0001$ ) (Figure 3C), and 2-fold higher when normalized to  $\beta$ -actin levels ( $p<0.0001$ ). Total protein concentration was 8-fold higher in the liver samples than the AT samples ( $p<0.0001$ ). Thus, per milligram of tissue, the concentration of *PNPLA3* was 3-fold higher in the liver than in AT ( $p<0.0001$ ) (Figure 3D). We estimated whole-body levels of *PNPLA3* in AT and the liver by multiplying the concentration of *PNPLA3* per milligram of tissue by the estimated organ weight. Average liver mass was 2.3±0.2 kg, and average AT mass was 54.4±2.9 kg. Assuming homogenous levels of *PNPLA3* in the liver and in AT depots, whole-body levels of *PNPLA3* were 9-fold higher in AT than the liver ( $p<0.0001$ ) (Figure 3E).

## DISCUSSION

The present series of studies were undertaken to investigate whether the PNPLA3-I148M variant changes AT TG composition as it does in the liver. Since this was found to be the case, we next determined whether this change in AT composition was reflected in AT FA composition, *in vivo* AT lipolysis, or the composition of fasting serum NEFAs released from AT. As previously reported for the liver lipidome in the same volunteers<sup>6</sup>, the I148M variant was associated with a more polyunsaturated TG composition of AT, while not influencing the rate of AT lipolysis or the composition of NEFAs released from AT. We found human AT to contain approximately 9-fold more PNPLA3 protein than the liver at the level of the whole body.

Polyunsaturated TGs were enriched in both absolute and relative terms in the *PNPLA3*<sup>I148M/MI</sup> compared with the *PNPLA3*<sup>I148I</sup> group when we profiled the AT lipidome from biopsies of 125 volunteers (Figure 1). This marked increase in polyunsaturated TG species in AT closely resembles our previous findings in the liver lipidome of mostly the same volunteers, which was also enriched with polyunsaturated TGs in I148M variant carriers compared with non-carriers<sup>6</sup>. Although UHPLC-QTOF-MS has a high detection sensitivity and is capable of detecting sub-ppm masses, this method only measures the total mass and the number of double bonds of individual TGs. To investigate the relative amounts of specific FA constituents in AT TGs, we conducted a further GC analysis of AT needle biopsies from 50 homozygous volunteers. These data essentially confirmed the changes seen in TG composition, indicating an accumulation of PUFAs in AT of PNPLA3-I148M carriers (Supplementary Figure 2 and Supplementary Figure 3).

We have recently shown, with the use of stable isotope FA tracers that the PNPLA3-I148M variant causes retention of PUFAs in TGs and a concomitant deficiency of polyunsaturated phosphatidylcholines (PCs) in the human liver<sup>7</sup>. This was also observed *in vitro* in stable human cell lines where incubation of cells with PUFAs induced lipid droplet accumulation in both homozygous PNPLA3-I148M knock-in and PNPLA3 knock-out cells but not in wild-type cells<sup>7</sup>. These data are similar to those by Mitsche *et al.* in knock-in mice expressing the catalytically inactive S47A allele<sup>8</sup>. In the latter study, it was proposed that PNPLA3 normally acts as a transacylase and transfers PUFAs from TGs to

PCs. The absence of this function in the PNPLA3-S47A knock-in mice apparently resulted in an enrichment of their livers with PUFA-containing TGs and a deficiency of PUFA-containing PCs. These data would support the idea that PNPLA3-I148M is a loss-of-function mutation in humans. Consistent with retention of PUFAs in the liver, PUFAs are also deficient in VLDL which transfers TG-bound FAs into AT and other peripheral tissues<sup>7</sup>. Thus, the excess of polyunsaturated TGs in AT cannot be secondary to their transfer from the liver to AT in VLDL.

Adipose tissue is chronically inflamed in obese subjects, which may contribute to insulin resistance and the development of NAFLD<sup>36-38</sup>. We have previously shown that AT inflammation is absent in PNPLA3-I148M carriers with NAFLD compared with non-carriers and suggested that this may contribute to the lack of insulin resistance in carriers of PNPLA3-I148M<sup>39</sup>. In the present study, the omega-6- to omega-3-PUFA ratio was lower in AT of carriers versus non-carriers of PNPLA3-I148M, reflecting lower concentrations of omega-6 AA and higher concentrations of omega-3 DPA (Supplementary Figure 2). Expression of anti-inflammatory genes were increased and proinflammatory genes unchanged in variant carriers compared with non-carriers. These changes are anti- rather than proinflammatory. Arachidonic acid is a precursor of eicosanoids that mediate the production of pro-inflammatory cytokines<sup>40</sup>, while DPA is synthesized from a precursor of anti-inflammatory eicosanoids<sup>40</sup>. An increased omega-6 to omega-3 ratio is associated with proinflammatory states and impaired function of metabolically active tissues such as the liver and AT<sup>40</sup>. The present data thus suggest that carriers of the PNPLA3-I148M variant possess metabolically healthy, PUFA-enriched AT that does not harbor pro-inflammatory properties. NAFLD caused by the I148M variant may also be protective against cardiovascular sequelae<sup>41-44</sup>. Interestingly, AT enriched with PUFA was shown in the Scottish Heart Health Extended Cohort study to decrease the risk of future cardiovascular events, independent of other known risk factors<sup>45</sup>.

The composition of subcutaneous AT is affected by long-term changes in dietary FA intake<sup>46</sup>. A limitation of this study is that we did not have dietary data available on the volunteers in whom lipidomic analyses of AT were conducted. We did, however, obtain careful dietary records in a recent study in which we demonstrated retention of PUFAs in

the liver of PNPLA3-I148M carriers<sup>7</sup>. In this study, the changes in PUFA metabolism were entirely attributed to the PNPLA3 genotype rather than diet. The changes in AT TGs in the present study closely mirror those seen in the liver. Thus, it is unlikely that the PUFA enrichment in AT would be due to dietary differences between the groups.

Rates of *in vivo* lipolysis measured in the basal state and during euglycemic hyperinsulinemia using [<sup>2</sup>H<sub>5</sub>]glycerol were similar in the *PNPLA3*<sup>148MM</sup> and *PNPLA3*<sup>148II</sup> groups (Figure 2). This analysis had 80% power to detect a 14% between-group difference in insulin suppression of glycerol R<sub>a</sub>. The turnover rates of individual FAs differ significantly<sup>47</sup>, which is why we used [<sup>2</sup>H<sub>5</sub>]glycerol rather than an individual FA such as <sup>13</sup>C-palmitate to trace lipolysis. We also determined the composition of circulating NEFAs in 125 volunteers, since changes in the AT lipidome would be expected to reflect serum NEFA composition in the fasted state. We found no significant differences in serum NEFAs between the *PNPLA3*<sup>148II</sup> and *PNPLA3*<sup>148MM/MI</sup> groups (Supplementary Table 5). Overall, these data imply that the increase in polyunsaturated IHTGs in I148M variant carriers is not due to increased NEFA delivery from AT to the liver.

Because we unexpectedly found the AT lipid composition to differ between carriers and non-carriers of the PNPLA3-I148M variant, we compared gene and protein expression of PNPLA3 between liver and AT samples in a small subset of the volunteers. *PNPLA3* mRNA was markedly higher in the human liver than in subcutaneous AT (Figure 3), consistent with previous studies<sup>15,16</sup>. This is in stark contrast to mice in which *PNPLA3* mRNA expression is unequivocally highest in AT depots and only small amounts of mRNA can be detected in other tissues, including the liver<sup>12-14</sup>. These contradictory results between human and mouse studies are yet to be explained but may reflect physiological differences between species. Despite higher gene expression in the liver, the PNPLA3 protein was much more abundant in AT than the liver (Figure 3). Importantly, we extrapolated AT protein expression from one subcutaneous AT biopsy to the whole body which assumes homogenous expression in all compartments of these tissues. This finding challenges the previous liver-centric view of the protein and its function in humans and raises the question as to whether polymorphisms in PNPLA3 could introduce significant alterations in human lipid metabolism via extrahepatic pathways.

We conclude that the PNPLA3 protein is found not only in the human liver, but also highly abundantly in AT. This is contrary to previous assumptions, according to which PNPLA3 is a liver-specific protein in humans. The PNPLA3-I148M variant alters AT lipid composition in a similar fashion as in the liver<sup>6</sup>, i.e., the lipidome is significantly enriched with polyunsaturated TGs. This change in AT lipid composition cannot explain the higher polyunsaturated IHTG content in PNPLA3-I148M carriers, since the variant does not affect the rate of AT lipolysis or the composition of NEFAs released from AT. We propose that the PNPLA3-I148M variant remodels TG composition in both the liver and AT independently, with the enrichment of PUFAs. This human knowledge is relevant as efforts are currently ongoing to develop novel pharmaceuticals to treat NAFLD caused by PNPLA3-I148M<sup>17-19</sup>. On the basis of our findings, we suggest that therapies aimed at ameliorating NAFLD due to PNPLA3-I148M should be liver-specific.

## REFERENCES

1. Romeo S, Kozlitina J, Xing C, et al. Genetic variation in PNPLA3 confers susceptibility to nonalcoholic fatty liver disease. *Nat Genet.* 2008;40(12):1461-1465.
2. Sookoian S, Pirola CJ. Meta-analysis of the influence of I148M variant of patatin-like phospholipase domain containing 3 gene (PNPLA3) on the susceptibility and histological severity of nonalcoholic fatty liver disease. *Hepatology.* 2011;53(6):1883-1894.
3. Romeo S, Sentinelli F, Cambuli VM, et al. The 148M allele of the PNPLA3 gene is associated with indices of liver damage early in life. *J Hepatol.* 2010;53(2):335-338.
4. Hyysalo J, Mannisto VT, Zhou Y, et al. A population-based study on the prevalence of NASH using scores validated against liver histology. *J Hepatol.* 2014;60(4):839-846.
5. Trepo E, Romeo S, Zucman-Rossi J, Nahon P. PNPLA3 gene in liver diseases. *J Hepatol.* 2016;65(2):399-412.
6. Luukkonen PK, Zhou Y, Sadevirta S, et al. Hepatic ceramides dissociate steatosis and insulin resistance in patients with non-alcoholic fatty liver disease. *J Hepatol.* 2016;64(5):1167-1175.
7. Luukkonen PK, Nick A, Holtta-Vuori M, et al. Human PNPLA3-I148M variant increases hepatic retention of polyunsaturated fatty acids. *JCI Insight.* 2019;4(16).
8. Mitsche MA, Hobbs HH, Cohen JC. Patatin-like phospholipase domain-containing protein 3 promotes transfer of essential fatty acids from triglycerides to phospholipids in hepatic lipid droplets. *J Biol Chem.* 2018;293(18):6958-6968.
9. Donnelly KL, Smith CI, Schwarzenberg SJ, Jessurun J, Boldt MD, Parks EJ. Sources of fatty acids stored in liver and secreted via lipoproteins in patients with nonalcoholic fatty liver disease. *J Clin Invest.* 2005;115(5):1343-1351.
10. Baulande S, Lasnier F, Lucas M, Pairault J. Adiponutrin, a transmembrane protein corresponding to a novel dietary- and obesity-linked mRNA specifically expressed in the adipose lineage. *J Biol Chem.* 2001;276(36):33336-33344.

11. Polson DA, Thompson MP. Adiponutrin mRNA expression in white adipose tissue is rapidly induced by meal-feeding a high-sucrose diet. *Biochem Biophys Res Commun.* 2003;301(2):261-266.
12. Lake AC, Sun Y, Li JL, et al. Expression, regulation, and triglyceride hydrolase activity of Adiponutrin family members. *J Lipid Res.* 2005;46(11):2477-2487.
13. Kershaw EE, Hamm JK, Verhagen LA, Peroni O, Katic M, Flier JS. Adipose triglyceride lipase: function, regulation by insulin, and comparison with adiponutrin. *Diabetes.* 2006;55(1):148-157.
14. Villena JA, Roy S, Sarkadi-Nagy E, Kim KH, Sul HS. Desnutrin, an adipocyte gene encoding a novel patatin domain-containing protein, is induced by fasting and glucocorticoids: ectopic expression of desnutrin increases triglyceride hydrolysis. *J Biol Chem.* 2004;279(45):47066-47075.
15. Wilson PA, Gardner SD, Lambie NM, Commans SA, Crowther DJ. Characterization of the human patatin-like phospholipase family. *J Lipid Res.* 2006;47(9):1940-1949.
16. Huang Y, He S, Li JZ, et al. A feed-forward loop amplifies nutritional regulation of PNPLA3. *Proc Natl Acad Sci U S A.* 2010;107(17):7892-7897.
17. BasuRay S, Wang Y, Smagris E, Cohen JC, Hobbs HH. Accumulation of PNPLA3 on lipid droplets is the basis of associated hepatic steatosis. *Proc Natl Acad Sci U S A.* 2019;116(19):9521-9526.
18. Linden D, Ahnmark A, Pingitore P, et al. Pnpla3 silencing with antisense oligonucleotides ameliorates nonalcoholic steatohepatitis and fibrosis in Pnpla3 I148M knock-in mice. *Mol Metab.* 2019;22:49-61.
19. Kumashiro N, Yoshimura T, Cantley JL, et al. Role of patatin-like phospholipase domain-containing 3 on lipid-induced hepatic steatosis and insulin resistance in rats. *Hepatology.* 2013;57(5):1763-1772.
20. Kotronen A, Peltonen M, Hakkarainen A, et al. Prediction of non-alcoholic fatty liver disease and liver fat using metabolic and genetic factors. *Gastroenterology.* 2009;137(3):865-872.
21. Bian H, Hakkarainen A, Zhou Y, Lundbom N, Olkkonen VM, Yki-Jarvinen H. Impact of non-alcoholic fatty liver disease on liver volume in humans. *Hepatol Res.* 2015;45(2):210-219.

22. Brunt EM, Janney CG, Di Bisceglie AM, Neuschwander-Tetri BA, Bacon BR. Nonalcoholic steatohepatitis: a proposal for grading and staging the histological lesions. *Am J Gastroenterol*. 1999;94(9):2467-2474.
23. Yki-Jarvinen H, Taskinen MR, Koivisto VA, Nikkila EA. Response of adipose tissue lipoprotein lipase activity and serum lipoproteins to acute hyperinsulinaemia in man. *Diabetologia*. 1984;27(3):364-369.
24. Folch J, Lees M, Sloane Stanley GH. A simple method for the isolation and purification of total lipides from animal tissues. *J Biol Chem*. 1957;226(1):497-509.
25. Burdge GC, Wright P, Jones AE, Wootton SA. A method for separation of phosphatidylcholine, triacylglycerol, non-esterified fatty acids and cholesterol esters from plasma by solid-phase extraction. *Br J Nutr*. 2000;84(5):781-787.
26. Evans K, Burdge GC, Wootton SA, Clark ML, Frayn KN. Regulation of dietary fatty acid entrapment in subcutaneous adipose tissue and skeletal muscle. *Diabetes*. 2002;51(9):2684-2690.
27. Castillo S, Mattila I, Miettinen J, Oresic M, Hyotylainen T. Data analysis tool for comprehensive two-dimensional gas chromatography/time-of-flight mass spectrometry. *Anal Chem*. 2011;83(8):3058-3067.
28. Sevastianova K, Kotronen A, Gastaldelli A, et al. Genetic variation in PNPLA3 (adiponutrin) confers sensitivity to weight loss-induced decrease in liver fat in humans. *The American journal of clinical nutrition*. 2011;94(1):104-111.
29. Nurjhan N, Campbell PJ, Kennedy FP, Miles JM, Gerich JE. Insulin dose-response characteristics for suppression of glycerol release and conversion to glucose in humans. *Diabetes*. 1986;35(12):1326-1331.
30. Ryysy L, Hakkinen AM, Goto T, et al. Hepatic fat content and insulin action on free fatty acids and glucose metabolism rather than insulin absorption are associated with insulin requirements during insulin therapy in type 2 diabetic patients. *Diabetes*. 2000;49(5):749-758.
31. Kotronen A, Vehkavaara S, Seppala-Lindroos A, Bergholm R, Yki-Jarvinen H. Effect of liver fat on insulin clearance. *Am J Physiol Endocrinol Metab*. 2007;293(6):E1709-1715.



32. Perttilä J, Huaman-Samanez C, Caron S, et al. PNPLA3 is regulated by glucose in human hepatocytes, and its I148M mutant slows down triglyceride hydrolysis. 2012;302(9):E1063-E1069.
33. Hochberg Y, Benjamini Y. More powerful procedures for multiple significance testing. *Stat Med*. 1990;9(7):811-818.
34. Luukkonen PK, Sadevirta S, Zhou Y, et al. Saturated Fat Is More Metabolically Harmful for the Human Liver Than Unsaturated Fat or Simple Sugars. *Diabetes Care*. 2018;41(8):1732-1739.
35. Faul F, Erdfelder E, Lang AG, Buchner A. G\*Power 3: a flexible statistical power analysis program for the social, behavioral, and biomedical sciences. *Behav Res Methods*. 2007;39(2):175-191.
36. Xu H, Barnes GT, Yang Q, et al. Chronic inflammation in fat plays a crucial role in the development of obesity-related insulin resistance. *J Clin Invest*. 2003;112(12):1821-1830.
37. Weisberg SP, McCann D, Desai M, Rosenbaum M, Leibel RL, Ferrante AWJ. Obesity is associated with macrophage accumulation in adipose tissue. 2003;112(12):1796-1808.
38. Tordjman J, Divoux A, Prifti E, et al. Structural and inflammatory heterogeneity in subcutaneous adipose tissue: relation with liver histopathology in morbid obesity. *J Hepatol*. 2012;56(5):1152-1158.
39. Lallukka S, Sevastianova K, Perttilä J, et al. Adipose tissue is inflamed in NAFLD due to obesity but not in NAFLD due to genetic variation in PNPLA3. *Diabetologia*. 2013;56(4):886-892.
40. Scorletti E, Byrne CD. Omega-3 fatty acids, hepatic lipid metabolism, and nonalcoholic fatty liver disease. *Annu Rev Nutr*. 2013;33:231-248.
41. Liu DJ, Peloso GM, Yu H, et al. Exome-wide association study of plasma lipids in >300,000 individuals. *Nat Genet*. 2017;49(12):1758-1766.
42. Simons N, Isaacs A, Koek GH, Kuc S, Schaper NC, Brouwers M. PNPLA3, TM6SF2, and MBOAT7 Genotypes and Coronary Artery Disease. *Gastroenterology*. 2017;152(4):912-913.

- Accepted Article
43. Xia MF, Lin HD, Chen LY, et al. The PNPLA3 rs738409 C>G variant interacts with changes in body weight over time to aggravate liver steatosis, but reduces the risk of incident type 2 diabetes. *Diabetologia*. 2019;62(4):644-654.
  44. Meffert PJ, Repp KD, Volzke H, et al. The PNPLA3 SNP rs738409:G allele is associated with increased liver disease-associated mortality but reduced overall mortality in a population-based cohort. *J Hepatol*. 2018;68(4):858-860.
  45. Woodward M, Tunstall-Pedoe H, Batty GD, Tavendale R, Hu FB, Czernichow S. The prognostic value of adipose tissue fatty acids for incident cardiovascular disease: results from 3944 subjects in the Scottish Heart Health Extended Cohort Study. *Eur Heart J*. 2011;32(11):1416-1423.
  46. Hodson L, Skeaff CM, Fielding BA. Fatty acid composition of adipose tissue and blood in humans and its use as a biomarker of dietary intake. *Prog Lipid Res*. 2008;47(5):348-380.
  47. Hagenfeldt L. Turnover of individual free fatty acids in man. *Fed Proc*. 1975;34(13):2246-2249.

# TABLES

**Table 1.** Clinical characteristics of the study volunteers.

Variable	AT and serum lipidome (n=125)		In vivo AT lipolysis (n=28)	
	<i>PNPLA3</i> <sup>148II</sup> (n=62)	<i>PNPLA3</i> <sup>148MM/MI</sup> (n=63)	<i>PNPLA3</i> <sup>148II</sup> (n=19)	<i>PNPLA3</i> <sup>148MM</sup> (n=9)
Age, years	46.4 ± 1.2	49.5 ± 1.0 *	50.6 ± 2.4	48.1 ± 4.1
Men	17 (27)	22 (35)	6 (32)	2 (22)
BMI, kg/m <sup>2</sup>	45.2 ± 0.7	45.4 ± 0.7	30.3 ± 1.1	30.6 ± 2.2
Waist, cm	129.2 ± 1.9	132.0 ± 1.8	98.4 ± 2.8	95.6 ± 5.3
Waist-to-hip ratio	0.93 (0.88-1.00)	0.97 (0.89-1.03)	0.89 (0.88-0.96)	0.88 (0.82-0.95)
SBP, mmHg	132 (122-144)	135 (124-146)	133 (114-145)	131 (123-150)
DBP, mmHg	89 (82-94)	92 (84-98)	81 (75-84)	92 (88-97) ***
Body fat, %	50 (48-54)	49 (44-54)	34 (26-43)	36 (26-38)
fP-Glucose, mmol/l	5.8 (5.1-6.4)	5.7 (5.2-6.4)	5.8 (5.1-6.0)	5.5 (5.2-5.9)
HbA <sub>1c</sub> , %	5.7 (5.5-6.3)	5.9 (5.5-6.2)	5.7 (5.3-6.0)	5.7 (5.4-5.9)
HbA <sub>1c</sub> , mmol/mol	38.8 (36.6-45.4)	39.9 (36.6-44.3)	38.3 (34.4-42.1)	38.8 (35.5-40.7)
fS-Insulin, mU/l	11.8 (7.9-17.1)	12.4 (6.5-18.3)	12.4 (4.1-16.9)	8 (6-12)
fP-HDL cholesterol, mmol/l	1.1 (0.9-1.4)	1.1 (1.0-1.3)	1.5 (1.3-1.9)	1.4 (1.1-1.8)
fP-LDL cholesterol, mmol/l	2.5 ± 0.1	2.5 ± 0.1	3.2 ± 0.2	3.1 ± 0.4
fP-Triglycerides, mmol/l	1.29 (0.96-1.67)	1.28 (1.01-1.62)	1.14 (0.74-1.48)	0.91 (0.79-1.64)
P-ALT, U/l	30 (24-39)	36 (26-46)	30 (16-36)	24 (22-61)
P-AST, U/l	28 (24-33)	32 (26-40) *	25 (22-31)	27 (25-43)
P-GGT, U/l	28 (19-43)	33 (22-48)	25 (19-53)	18 (14-51)
P-Albumin (g/l)	38 ± 0.4	38 ± 0.3	40 ± 0.5	39 ± 1.2
B-Platelets (10 <sup>9</sup> /l)	252 (209-303)	233 (202-285)	253 (221-271)	240 (226-266)
P-Creatinine, μmol/l	67 (58-74)	64 (57-73)	73 (62-75)	76 (61-83)
IHTG, %	5 (0-20)	15 (5-30)	14 (5-31)	24 (20-33)
<i>PNPLA3</i> (CC/CG/GG), n	62/0/0	0/57/6 ***	19/0/0	0/0/9 ***
NASH	7 (11)	16 (25) *	NA	NA
Type 2 diabetes	25 (40)	33 (52)	0	0
Use of statins	22 (35)	18 (29)	1 (5)	2 (22)

Data are in n (%), mean ± SEM or median (25<sup>th</sup> – 75<sup>th</sup> percentiles). Statistical tests used are the unpaired two-tailed Student's *t* test, Mann-Whitney *U* test, Pearson's  $\chi^2$  test, or the Fisher's exact test, as appropriate. SBP, systolic blood pressure; DBP, diastolic blood pressure; IHTG, intrahepatic triglycerides. \**p*≤0.05, \*\*\**p*≤0.001

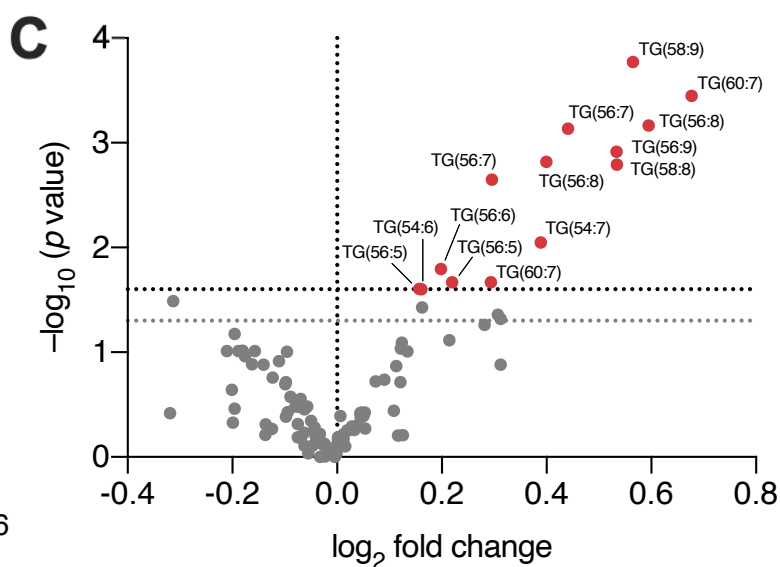
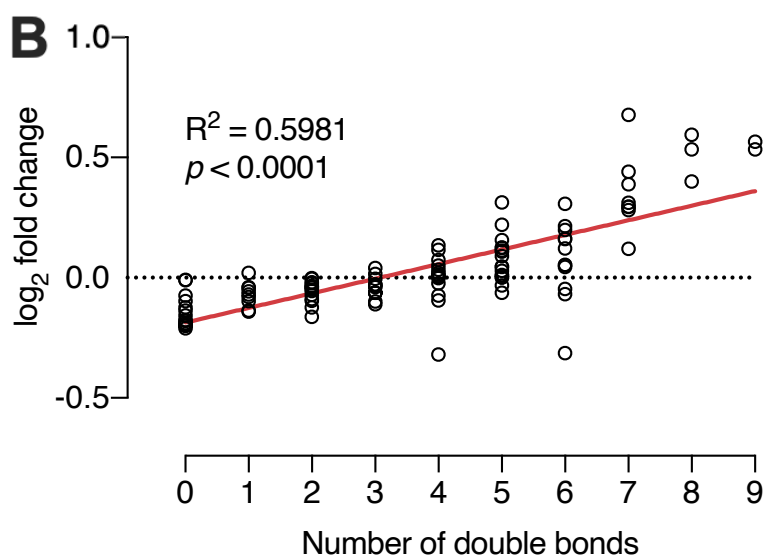
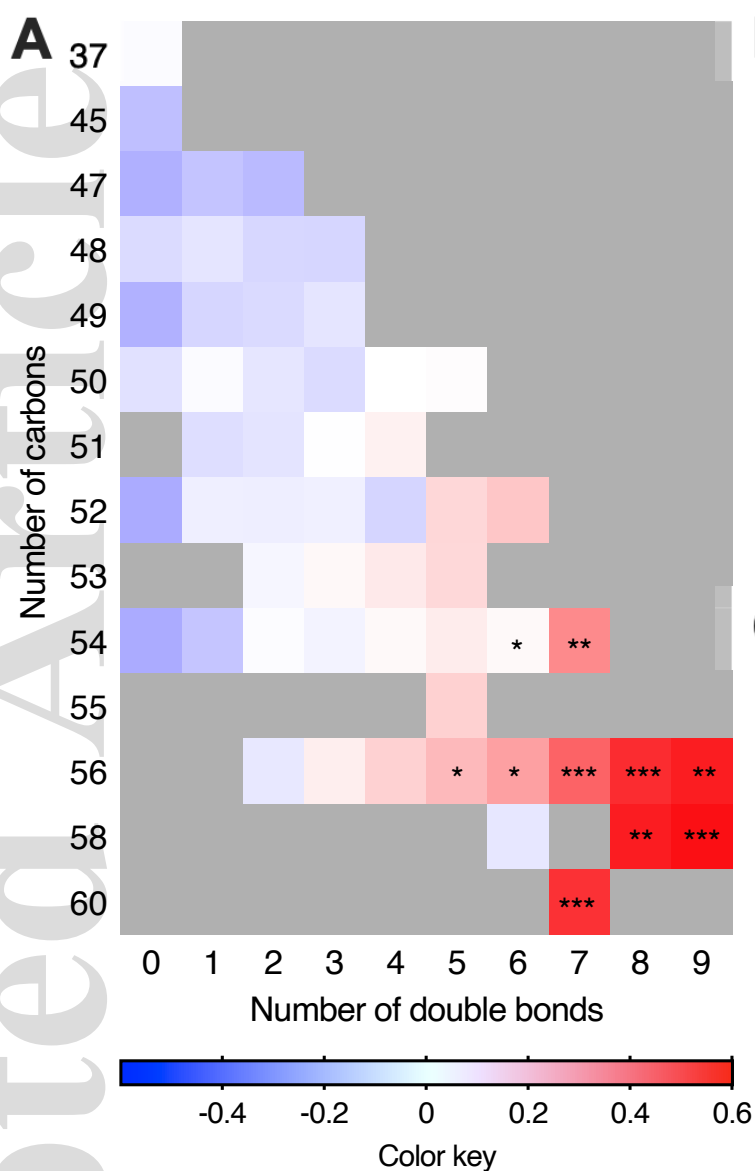
## TABLES

## FIGURES AND FIGURE LEGENDS

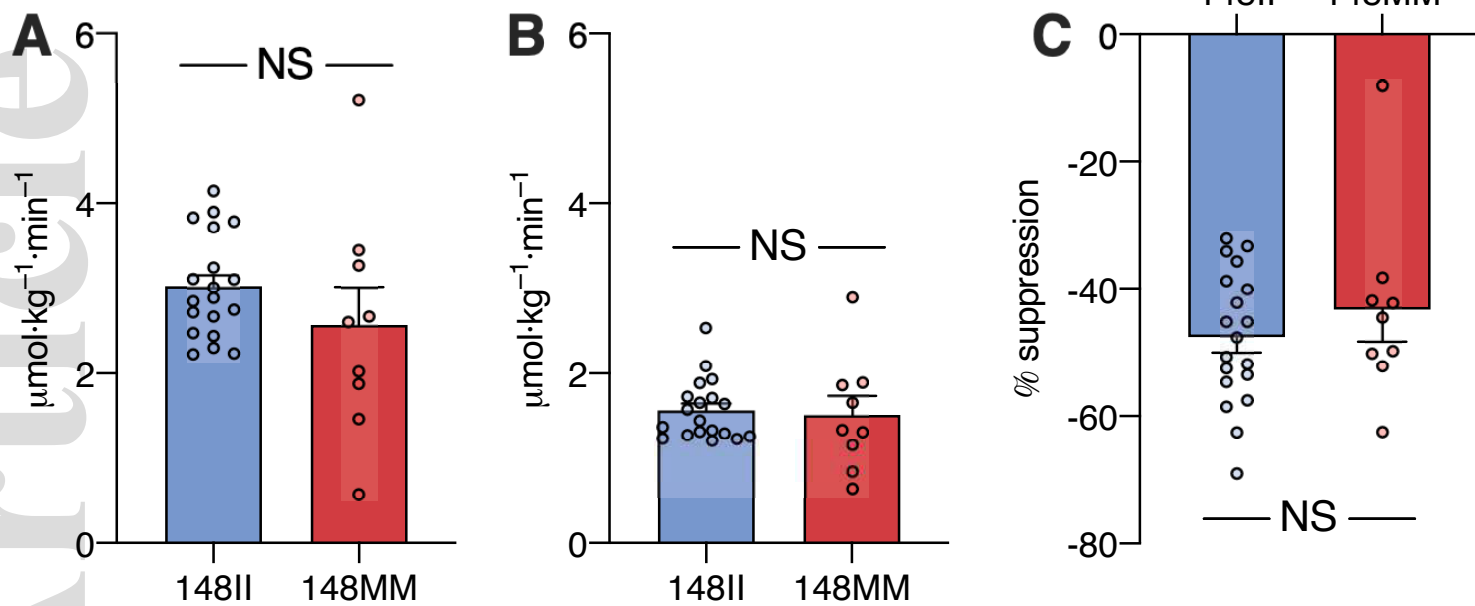
**Figure 1. Adipose tissue TGs are enriched with PUFAs in PNPLA3-I148M variant carriers compared with non-carriers.** (A) Heatmap showing differences in absolute concentrations of various TG species in AT of the *PNPLA3*<sup>148MM/MI</sup> group ( $n=63$ ) compared with the *PNPLA3*<sup>148II</sup> group ( $n=62$ ). The x-axis denotes the number of double bonds and the y-axis the number of carbons in a TG molecule. Color coding represents  $\log_2$  of the fold change in TG concentrations between the groups. The brighter the red color, the higher the increase in the absolute concentration of a TG species in the *PNPLA3*<sup>148MM/MI</sup> group compared with the *PNPLA3*<sup>148II</sup> group. The unpaired two-sample Student's *t*-test and the Benjamini-Hochberg method for multiple testing were applied to determine significance after log-transformation of the data.  $*p \leq 0.05$ ,  $**p \leq 0.01$ ,  $***p \leq 0.001$ . (B) Linear regression between the number of double bonds in TGs and the  $\log_2$  of the fold change in absolute concentrations of corresponding TGs between *PNPLA3*<sup>148MM/MI</sup> and *PNPLA3*<sup>148II</sup> groups. (C) A volcano plot showing changes in individual TGs in the *PNPLA3*<sup>148MM/MI</sup> group compared with the *PNPLA3*<sup>148II</sup> group. The x-axis denotes  $\log_2$  of the fold change in the concentration of a given TG species between the groups, and the y-axis denotes negative  $\log_{10}$  of the *p* value of an unpaired two-sample Student's *t*-test comparing concentrations of a given TG between the groups. The lower gray horizontal dotted line represents  $p=0.05$ , and the upper black horizontal dotted line represents the minimum level of Benjamini-Hochberg corrected significance. Red dots denote significantly increased TGs, which are labeled.

**Figure 2. The PNPLA3-I148M variant does not affect the rate or insulin suppression of AT lipolysis.** Glycerol  $R_a$  in the *PNPLA3*<sup>148II</sup> (blue bars,  $n=19$ ) and *PNPLA3*<sup>148MM</sup> (red bars,  $n=9$ ) groups in the basal state (A) and during euglycemic hyperinsulinemia (B), and the percentage suppression of glycerol  $R_a$  during the hyperinsulinemic clamp (C). Bars represent means  $\pm$  SEM. The unpaired two-sample Student's *t*-test was used to determine significance.

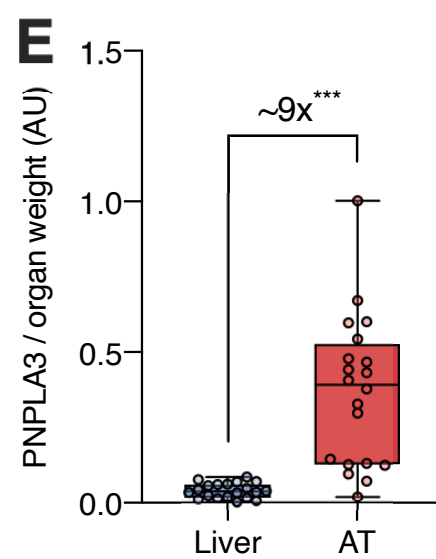
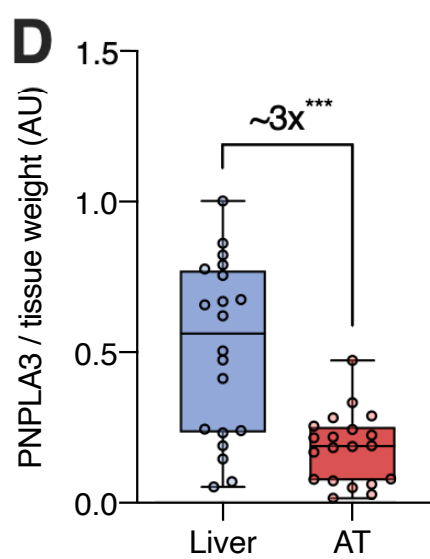
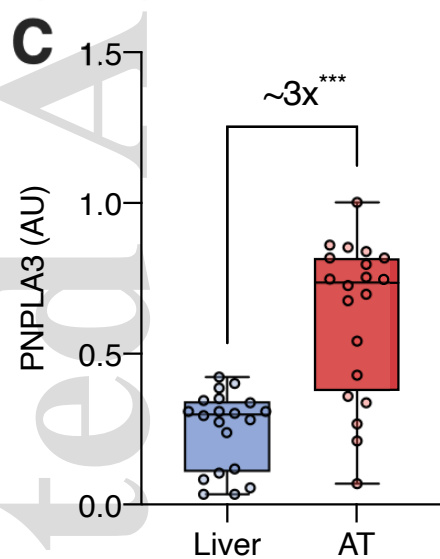
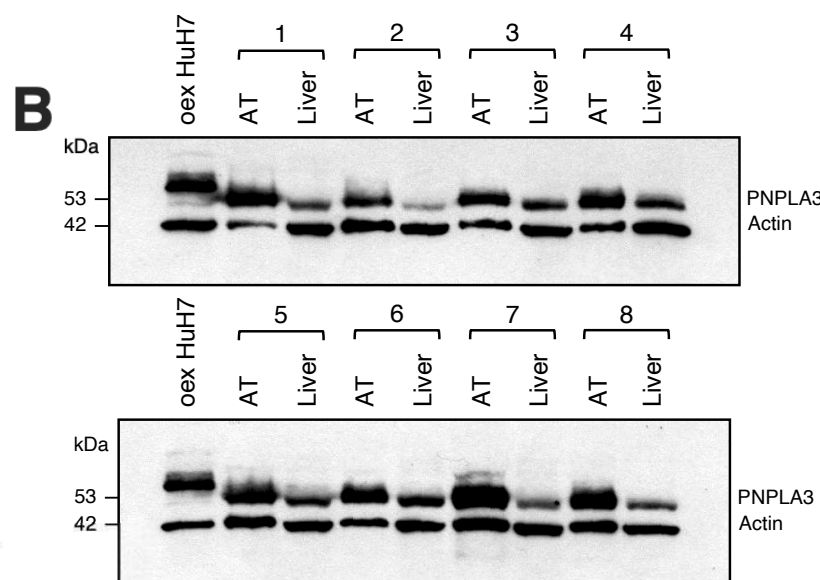
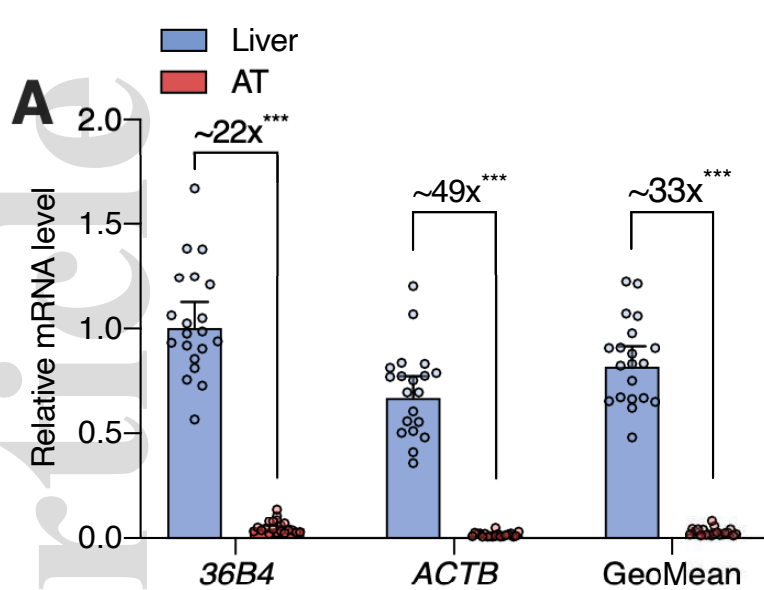
**Figure 3. PNPLA3 is found abundantly in human AT.** (A) Expression of *PNPLA3* mRNA in the human liver (blue bars,  $n=20$ ) and AT (red bars,  $n=20$ ) shown as means  $\pm$  95% confidence intervals. All measurements were performed twice. Expression data were normalized either to the housekeeping gene *36B4*, *ACTB*, or the geometric mean of their expression levels. Expression in the liver normalized to *36B4* was set to equal one. (B) Representative immunoblots from eight volunteers are shown. Positive controls from *PNPLA3*-overexpressing HuH7 cell lysates (oex HuH7) are shown in the first wells. The encoded protein has a slightly higher molecular mass than the endogenous *PNPLA3*, since it carries a His<sub>6</sub> tag and an Xpress antibody epitope. (C-E) *PNPLA3* protein levels in the human liver (blue boxes,  $n=20$ ) versus AT (red boxes,  $n=20$ ). Boxes show median as a horizontal line and the bounds of the boxes represent interquartile ranges. Whiskers extend to minimum and maximum values. Data are shown as either *PNPLA3* levels per milligram of tissue protein (C), per milligram of tissue (D), or as whole-body levels of *PNPLA3* (E) calculated by multiplying the amount of *PNPLA3* per milligram of tissue by the estimated organ weight. The paired two-sample Student's *t*-test was used to determine significance. \*\*\* $p \leq 0.001$ .



liv\_14507\_f1.eps



liv\_14507\_f2.eps



liv\_14507\_f3.eps